Molecular Crystals and Liquid Crystals
Publication details, including instructions for authors and subscription information:
http://www.tandfonline.com/loi/gmcl18

Fourier Transform Infrared Absorption Study of Hexa(hexylthio)triphenylene: A Discotic Liquid Crystal

W. K. Lee [a] , P. A. Heiney [a] , J. P. McCauley JR. [b] & A. B. Smith III [b]

[a] Department of Physics and Laboratory for Research on the Structure of Matter, University of Pennsylvania, Philadelphia, PA, 19104, U.S.A.

[b] Department of Chemistry and Laboratory for Research on the Structure of Matter, University of Pennsylvania, Philadelphia, PA, 19104, U.S.A.

Version of record first published: 24 Sep 2006.

To cite this article: W. K. Lee , P. A. Heiney , J. P. McCauley JR. & A. B. Smith III (1991): Fourier Transform Infrared Absorption Study of Hexa(hexylthio)triphenylene: A Discotic Liquid Crystal, Molecular Crystals and Liquid Crystals, 198:1, 273-284

To link to this article: http://dx.doi.org/10.1080/00268949108033403

Mol. Cryst. Liq. Cryst., 1991, Vol. 198, pp. 273–284
Reprints available directly from the publisher
Photocopying permitted by license only

Printed in the United States of America

Fourier Transform Infrared Absorption Study of Hexa(hexylthio)triphenylene: A Discotic Liquid Crystal

W. K. LEE and P. A. HEINEY

Department of Physics and Laboratory for Research on the Structure of Matter, University of Pennsylvania, Philadelphia, PA 19104, U.S.A.

and

J. P. MCCAULEY, JR. and A. B. SMITH, III

Department of Chemistry and Laboratory for Research on the Structure of Matter, University of Pennsylvania, Philadelphia, PA 19104, U.S.A.

(Received July 25, 1990)

We have used Fourier transform infrared absorption spectroscopy to study the molecular motions of hexa(hexylthio)triphenylene as a function of temperature. Our measurements show pronounced changes in the CH_3 stretching mode frequencies at the $K \rightarrow H$ transition. (The H phase displays long range incommensurate helical order). However, the CH_2 stretching mode frequencies show much less variation with temperature, suggesting that only the ends of the alkyl tails undergo much change in the different phases. The CH bending and benzene stretching vibrations show a change in the frequency-temperature dependence at both the $K \rightarrow H$ and the $H \rightarrow D_{hd}$ transitions. There is no observable change in the spectrum in going from the D_{hd} to the I phase. We also present detailed syntheses for hexa(hexylthio)triphenylene and its C5 and C7 homologs.
Physics Abstracts Classification: 64.70.M, 61.30.E, 33.20.E, 78.30.

Keywords: Discotic liquid crystal, infrared absorption, phase transition, HHTT

1. INTRODUCTION

Since their discovery[1] in 1977, many studies have been performed to elucidate the microscopic structure of discotic liquid crystals. X-ray diffraction measurements[2–7] have provided considerable information on the symmetry and long-range order of these fascinating systems. However, more microscopic information about detailed molecular conformations and disorder is crucial to understanding the mechanisms underlying discotic mesomorphism. The vast majority, if not all, of discotic mesogens possess 4–8 flexible aliphatic tails. Indirect evidence from X-ray studies[4,5] indicates that these tails may be quite disordered, and that this disorder may increase rapidly with increasing temperature. An alternate approach to examining

such short-range and intramolecular order is to use a more local probe such as Raman scattering,[11] NMR,[11-17] or infrared absorption.[11,18-21]

We have used Fourier Transform Infrared (FTIR) absorption to study the vibrational dynamics of hexa(hexylthio)triphenylene (HHTT) as a function of temperature. As discussed below, both crystalline and liquid crystalline structures of this material have been extensively characterized *via* X-ray diffraction. The object of the present study was to gain an understanding of the local conformations of the molecule in the various phases, and the role of tail disorder in stabilizing those phases. We have separately reported[22] a similar study of truxene based discotics, which show isotropic phase reentrancy and other surprising behavior. The present paper is the first study of molecular vibrations in HHTT, and to our knowledge the first infrared absorption study of any triphenylene derivative, although there have been several NMR studies of hexa-*n*-alkoxy derivatives of triphenylene.[12,13]

In the remainder of this section we summarize previous research on HHTT. In subsequent sections we will present detailed syntheses for HHTT and its C5 and C7 homologs, describe the methods used in the temperature-dependent infrared absorption studies, and finally discuss the results of those studies.

The first structural study of HHTT[23] revealed the following phase sequence:

$$K \underset{62C}{\longleftrightarrow} D_{ho} \underset{70C}{\longleftrightarrow} D_{hd} \underset{93C}{\longleftrightarrow} I$$

A more detailed X-ray diffraction study[6,7] revealed the following features of the various phases (Figure 1):

(i) The crystalline (K) phase has a monoclinic structure. The molecules are ordered into columns, within which there is a repeat unit of two molecules. The aliphatic tails are not confined to the plane of the core, but tilt up and down; two of the six tails contain isolated *gauche* bonds, resulting in considerable displacement of the end of the tail from the plane of the core. Substantial thermal motion is seen at the ends of the tails at room temperature.

(ii) The H phase, although crystalline, closely resembles liquid-crystalline columnar phases. (This phase was previously[6,7,23] referred to as "D_{ho}." However, this notation is generally taken to refer to a putative liquid crystal phase with long-range intracolumnar order, rather than a three-dimensional crystal with columnar order. Therefore, we have named the helically ordered phase the 'H' phase). Molecules are ordered into columns in a hexagonal array. Within each column adjacent molecules are rotated by ~45.5°, resulting in long range helical order with a pitch P equal to 7.92 molecular spacings, i.e. incommensurate with the positional order along the columns. (Similar *short-range* helical order has been observed in hexa-*n*-alkoxy derivatives of triphenylene and other columnar materials by Levelut *et al.*[8-10].) Furthermore, a three-column superlattice results from both the relative phases and signs of helices in different columns and also from the translations of molecules along the columns. In the modelling of this phase to fit the X-ray results it was assumed that the aliphatic tails were fully extended (with all *trans* bonds), but that the tails were tilted ± 3–$5°$ above and below the plane of the cores to form a "propellor" structure.

(iii) In the liquid crystalline D_{hd} phase, the molecules still form a hexagonal

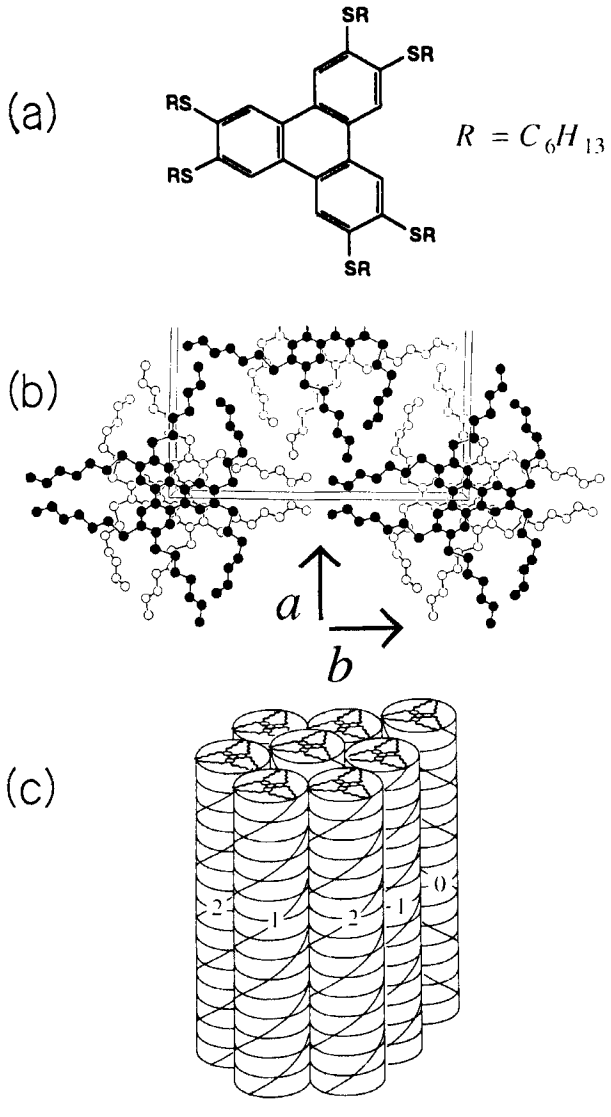

FIGURE 1 (a) Molecular structure of hexa(hexylthio)triphenylene (HHTT). (b) Crystal (*K*-phase) structure of HHTT.[7] Shown is the view of half of the unit cell, seen from the *c*-axis. Atoms in the upper plane are indicated with closed circles, atoms in the lower plane with open circles. (c) Model for structure of the *H* phase.[7] Column 0 has the opposite helicity from columns 1 and 2, and is displaced by $z = p/2$ from those columns, where p is the intracolumn molecular spacing.

array of columns. However, the positional order within the columns is liquidlike, and both helical and superlattice order is lost. Little is known about the quantitative extent of tail disorder in the HHTT D_{hd} phase. However, a linear decrease in the intercolumnar lattice constant with increasing temperature is consistent with a thermally activated increase in the density of *gauche* bonds.

(iv) Although the isotropic liquid (*I*) phase was not studied in detail, we can

infer from many other studies of discotic compounds that there is considerable nematic-like short-range order. It is plausible to assume that there is a high level of tail disorder in the *I* phase.

2. SYNTHESIS

The syntheses of the hexa-alkylthio substituted triphenylenes have been previously described.[25,26] The literature procedure for the preparation of these compounds is nucleophilic aromatic substitution of hexabromotriphenylene[27] with 12 equivalents of the sodium alkylthiolate, in the polar aprotic solvent DMEU, at 100°C, for 1 to 2 hours. The sodium thiolates are typically generated in ethanol from the thiols, using sodium ethoxide as a base, followed by concentration, washing of the solid residue with ether, filtration, and drying under vacuum.[28,29] Reported yields for the substitution reaction ranged from 40 to 55%. In our hands, this protocol resulted in substantial decomposition. Marked improvement was seen when the DMEU solution was heated to only 70°C for no more than 30 minutes. Also, the thiol salts were more conveniently generated in anhydrous form by treating the mercaptan with sodium hydride in ether and then simply removing the solvent *in vacuo*. These modifications not only enhanced the yield of the desired material (78–84%), but also greatly facilitated purification (i.e., less side products). A detailed experimental with full spectral characterization of the C5, C6, and C7 derivatives follows.

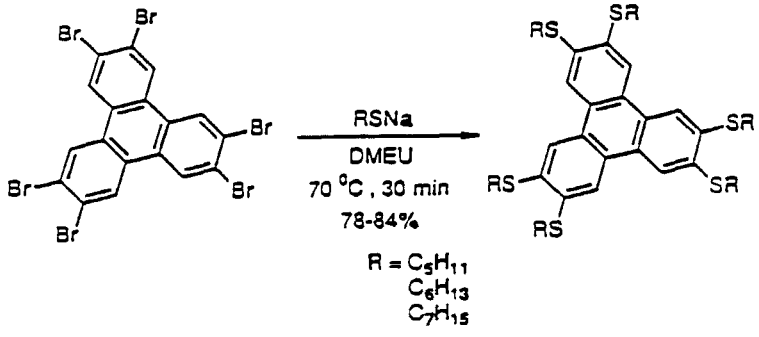

General Procedure for the Preparation of 2,3,6,7,10,11-Hexa(alkylthio)Triphenylenes

Into a 3 neck, 100 mL round bottom flask equipped with a reflux condenser, argon inlet, magnetic stirrer and rubber septa was placed 750 mg of a 60% dispersion in oil of sodium hydride (18.8 mmol, 13.1 equiv.). To this dispersion was added dry pentane (30 mL). The mixture was vigorously stirred, then allowed to stand. The pentane supernatant was next removed *via* cannula, and the sodium hydride washed twice more with pentane. Once the oil had been removed, the sodium hydride was suspended in 50 mL of dry ether. The flask was then cooled in an ice bath and the alkyl thiol (17.1 mmol, 12.0 equiv.) was added dropwise over 5 min. After the thiol had been completely added and hydrogen evolution was no longer evident, the ice bath was removed and the mixture heated to reflux for 15 min. At the end

of this time a colorless precipitate of the sodium alkyl thiolate was seen. After cooling, the ether was removed using a rotary evaporator, while maintaining an inert atmosphere. The resultant solid thiol salt was then suspended in 40 mL of dry DMEU (dimethylethylideneurea distilled from CaH_2). To this mixture was added 1.0 g of hexabromotriphenylene (1.43 mmol, 1.0 equiv.) prepared by the method of Breslow *et al.*[24] The mixture was then placed in an oil bath, which had been preheated to 70°C and stirred vigorously for 30 min. At the end of this period, all material had dissolved. The reaction was then cooled in an ice bath and 20 mL of water added. The mixture was trnasferred to a 500 mL separatory funnel and 100 mL of ether/CH_2Cl_2 (4:1) added. The organic layer was washed twice with 250 mL water, once with 75 mL brine, dried over Na_2SO_4, and concentrated *in vacuo*. The crude product was purified by recrystallization from ether/pentane or acetone to give the respective triphenylene derivative as colorless needles.

2,3,6,7,10,11-Hexa-(Pentylthio)-Triphenylene (84% yield) mp 93–94°C: IR($CHCl_3$) 3007 (m), 2979 (s), 2945 (s), 2880 (m), 1599 (m), 1460 (s), 1376 (m) cm^{-1}; ^1H NMR (500 MHz, $CDCl_3$) δ 0.94 (t, J = 7.1 Hz, 18 H), 1.36–1.44 (m, 12 H), 1.50–1.56 (m, 12 H), 1.80 (tt, J = 7.3 and 7.5 Hz, 12 H), 3.07 (t, J = 7.3 Hz, 12 H), 7.99 (s, 6 H); ^{13}C NMR (125 MHz, $CDCl_3$) δ 136.31, 126.66, 121.68, 33.49, 31.34, 28.39, 22.37, 13.98; high resolution mass spectrum (FAB) m/z 840.3980 [$(M)^+$; calcd for $C_{48}H_{72}S_6$: 840.3938].

2,3,6,7,10,11-Hexa-(Hexylthio)-Triphenylene (78% yield) mp 61–62°C (soften) 92–93°C (melt): IR ($CHCl_3$) 3003 (m), 2977 (s), 2943 (s), 2875 (s), 1595 (m), 1457 (s), 1373 (m) cm^{-1}; ^1H NMR (500 MHz, $CDCl_3$) δ 0.91 (t, J = 7.0 Hz, 18 H), 1.34–1.38 (m, 24 H), 1.52–1.58 (m, 12 H), 1.79 (tt, J = 7.3 and 7.5 Hz, 12 H), 3.07 (t, J = 7.3 Hz, 12 H), 7.98 (s, 6H); ^{13}C NMR (125 MHz, $CDCl_3$) δ 136.29, 126.62, 121.67, 33.55, 31.50, 28.80, 28.68, 22.56, 14.02; high resolution mass spectrum (FAB) m/z 924.4785 [$(M)^+$, calcd for $C_{54}H_{60}S_6$: 924.4897].

2,3,6,7,10,11-Hexa-(Heptylthio)-Triphenylene (80% yield) mp 72–73°C (soften) 93–94°C (melt): IR ($CHCl_3$) 2999 (m), 2975 (s), 2941 (s), 2878 (s), 1592 (m), 1453 (s), 1374 (m) cm^{-1}; ^1H NMR (500 MHz, $CDCl_3$), δ 0.89 (t, J = 6.9 Hz, 18 H), 1.28–1.34 (m, 24 H), 1.34–1.40 (m, 12 H), 1.51–1.57 (m, 12 H), 1.79 (tt, J = 7.3 and 7.4 Hz, 12 H), 3.06 (t, J = 7.3 Hz, 12 H), 7.88 (s, 6 H); ^{13}C NMR (125 MHz, $CDCl_3$) δ 136.08, 126.46, 121.33, 33.48, 31.76, 29.20, 29.03, 28.68, 22.62, 14.04; high resolution mass spectrum (FAB) m/z 1008.5890 [$(M)^+$, calcd for $C_{60}H_{96}S_6$: 1008.5836].

3. PHYSICAL MEASUREMENTS

About 10 mg of sample was dissolved in 0.4 mL of basic alumina filtered chloroform, and using a syringe a few drops of the solution were carefully deposited on a 25

mm diameter × 2 mm thick KBr disk. Argon gas was then blown over the drops to evaporate the chloroform. This was repeated two or three times until about 2 mg of pure sample was deposited on the KBr plate. The plate was then placed in a drying oven (~80°C) for several minutes to ensure complete evaporation of the chloroform. A 0.015 mm teflon gasket was placed on the plate and another KBr plate seated above it, forming the FTIR absorption cell. The cell was then placed in a Wilmad #118-3 temperature-controlled cell mount, which was connected to a Wilmad #0106 temperature controller. The temperature was stable to within 1°C. In order to get as uniform a thin film as possible, the sample cell was heated to about 100°C, while the cell mount was carefully screwed in place thereby pressing the two KBr plates together. In this way, the teflon gasket also formed a seal, preventing the sample from leaking. The sample was allowed to cool to room temperature before placing it in the sample compartment of the FTIR instrument. The sample compartment was purged with dried nitrogen gas for at least 3 hours before the start of data collection. The temperature inside the cell was separately calibrated with a thermistor embedded inside two KBr plates.

The measurements were done in transmission mode, on an IBM IR/97 FTIR spectrometer. A total of 128 scans were co-added to give a reasonable signal-to-noise ratio with a resolution of 0.5 cm^{-1}. The absorption spectrum was measured in the 400 to 4000 cm^{-1} region. Data were taken in 5°C increments by heating the sample from about 30°C to 141°C. A reference spectrum of empty KBr disks was taken and was used for subsequent computation of the absorption spectra. As a check, several spectra of the reference cell were taken at different temperatures ranging from 30°C to 175°C. There were no observable differences between these spectra.

Due to possible sample flow within the FTIR cell, we could not be sure that the IR beam passed through exactly the same amount of sample as the cell was heated. Therefore, in interpreting the results, we concentrated mainly on the frequency changes rather than the amplitude changes. In order to obtain a more quantitative description of these frequency variations, we fit our spectra to an empirical (but fixed) lineshape. The functional form chosen for the least squares fits was a sum of lorentzians plus a quadratic background function. To get a good fit, it was occasionally necessary to parameterize a single peak with more than one lorentzian. In these cases we quote the weighted average of the various sub-frequencies.

4. RESULTS

Figure 2 shows the complete FTIR absorption scans of HHTT taken at 29°C (*K* phase) and 141°C (*I* phase). Based on extensive literature on the subject, especially regarding *n*-alkanes,[30-33] several peaks are easily identified, as labelled: (a) CH stretching modes near 2900 cm^{-1}, (b) benzene breathing modes near 1600 cm^{-1}, (c) CH bending modes near 1380 and 1460 cm^{-1}, (d) single H out-of-plane bends of benzene near 870 cm^{-1}, and (e) CH rocking modes near 720 cm^{-1}. Although peaks in the region between 100–1300 cm^{-1} are mostly due to the twisting and wagging modes of the tails, due to the proximity of the modes, individual peaks

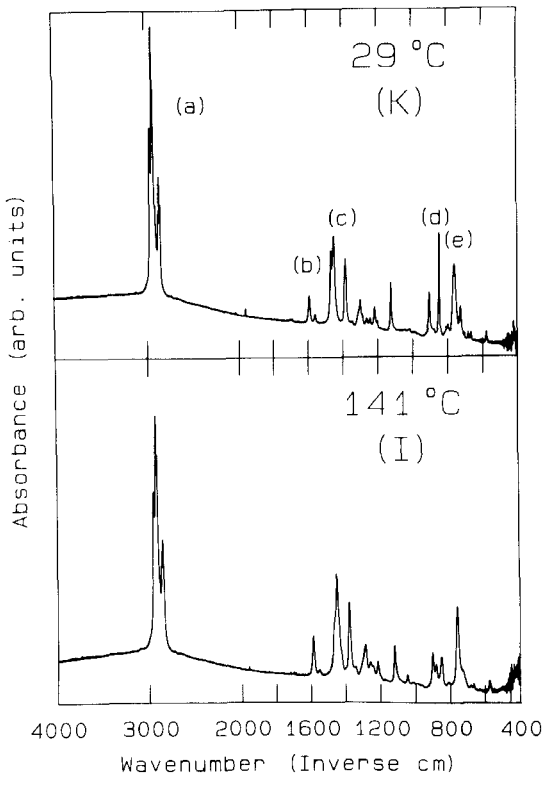

FIGURE 2 Complete FTIR absorption spectra of HHTT at (a) 29°C and (b) 141°C in arbitrary absorption units. The bands in the marked regions are assigned as follows: (a) methyl and methylene CH stretches, (b) benzene ring breathing modes, (c) methyl and methylene CH bends and scissoring, (d) out-of-plane deformation of aromatic hydrogen and (e) methylene rocking mode. Other bands had no definite assignments. Note the compressed scale from 4000 to 2000 cm^{-1}.

in that and the 600–800 cm^{-1} region could not be identified. The two spectra are qualitatively quite similar. With the exception of a few new peaks at higher temperatures, the principal effect of increasing the temperature is a decrease in peak amplitude and a broadening of individual lines, so that closely separated peaks become unresolved at high temperature.

Figure 3 shows the evolution of three selected regions in the IR spectra with increasing temperature: (a) CH bending/scissoring modes, (b) benzene stretching modes, and (c) CH stretching modes. The peaks are identified as follows: CH_3 symmetric bending mode at ~1380 cm^{-1}, CH_3 asymmetric bending mode at ~1450 cm^{-1}, CH_2 scissoring mode at ~1465 cm^{-1}, benzene stretching modes at ~1550 cm^{-1} and ~1590 cm^{-1}, CH_2 symmetric stretching mode at ~2853 cm^{-1}, CH_3 symmetric stretching mode at ~2875 cm^{-1}, CH_2 asymmetric stretching mode at ~2925 cm^{-1}, and CH_3 asymmetric stretching mode at ~2960 cm^{-1}. Clearly, there are both gradual and sudden amplitude and frequency changes with temperature.

Figure 4(a) shows the weighted average of the CH_3 symmetric bending absorption frequencies as a function of temperature. Although the effect is small, it is clear

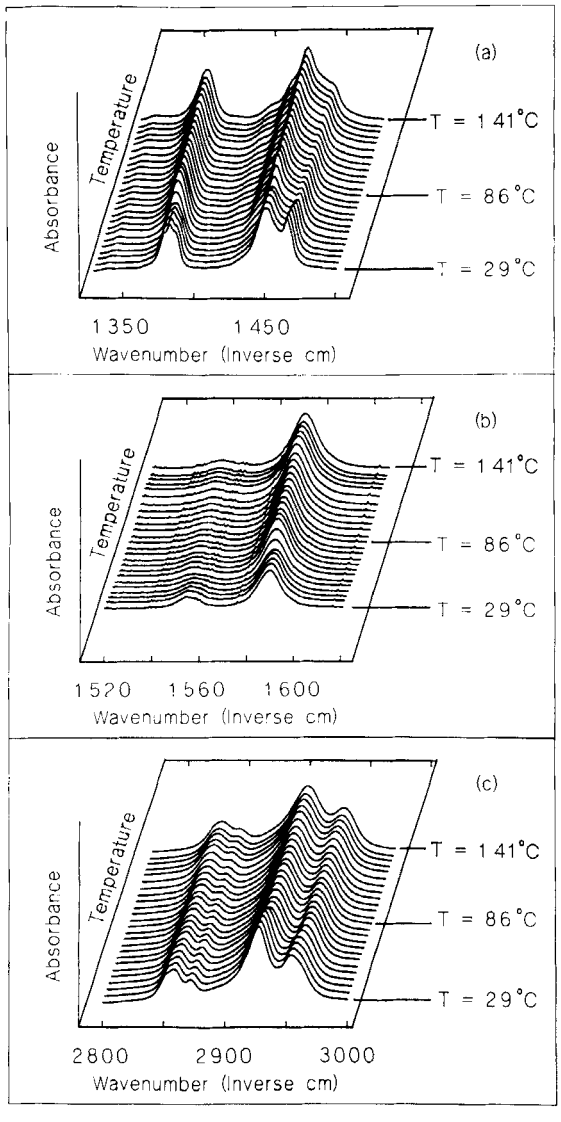

FIGURE 3 FTIR absorption profiles of (a) CH bending modes, (b) benzene stretching modes, and (c) CH stretching modes as a function of temperature. Data were taken upon heating at the following temperatures: 29, 33, 39, 43, 48, 53, 58, 63, 68, 72, 77, 81, 86, 91, 96, 100, 105, 109, 114, 118, 123, 127, 132, 136, and 141°C.

that the slope of frequency *vs.* temperature changes at around 50°C and 70°C. While the change at 70°C corresponds to the $H \rightarrow D_{hd}$ transition, the change at 50°C is actually about 12°C lower than the nominal melting point of 62°C. A similar change of slope is seen in Figure 4(b), where the frequency of a benzene ring stretching mode is plotted against temperature. Again, the slope changes at both 50°C and 70°C. Figure 4(c) shows the temperature dependence of the frequency of the asymmetric stretching mode of the CH_3 group at the end of the alkyl tails.

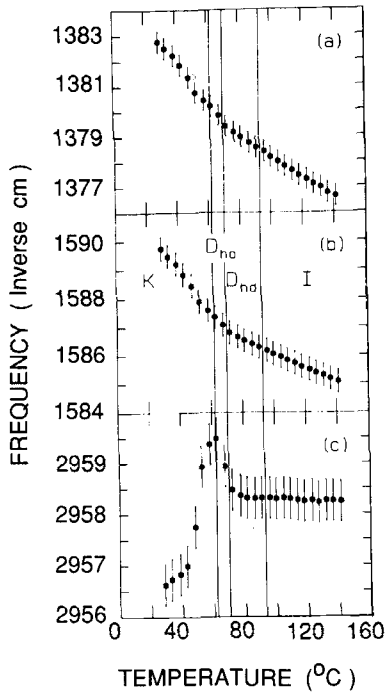

FIGURE 4 Fitted positions of the absorption peaks from lorentzian fits to data shown in Fig. 3. (a) methyl symmetric bending mode (b) benzene stretching mode (c) methyl group asymmetric CH stretching mode. In cases where more than one lorentzian were needed to give a reasonable fit, the weighted averaged of the positions are plotted. Error bars indicate estimated errors from the fits.

In this case, dramatic changes are seen at 50°C, 60°C, and 70°C. The symmetric stretching mode of CH_3 at around 2875 cm^{-1} (not plotted) shows the same behavior as its asymmetric counterpart. It is generally understood,[34,35] that CH_3 stretching mode frequencies are increased by the introduction of *gauche* bonds. Thus, a plausible source for the peak movement shown in Figure 4(c) is an increase in the statistical distribution of *gauche* bonds in the alkyl tails.

Analysis of these peak shifts is facilitated by detailed comparison with X-ray diffraction results. In the *K* phase, for which the crystal structure is known, four of the alkyl tails are fully extended, although they are somewhat tilted and distorted from an ideal conformation consisting of all *trans* (antiperiplanar) bonds, while two of the tails contain a single *gauche* bond.[7,24] The root-mean-square amplitudes of carbon-atom displacements range from less than 0.25 Å near the core of the molecule, to almost 0.50 Å near the ends of the tails. Models used in least-squares fits of the *H* phase X-ray diffraction data[6,7] assumed that the tails were fully extended, and this assumption is further strengthened by the observation that the intercolumnar distance in the *H* phase is temperature-independent. However, both the presence of diffuse off-axis scattering and calculated Debye-Waller factors indicated that a certain amount of tail disorder or at least tail vibrational motion is present. (Note that the incommensurate structure of the *H* phase implies that no two molecules find themselves in exactly identical environments). Diffuse scat-

tering is also seen in diffraction from the D_{hd} phase[7]; in addition, the intercolumnar distance decreases rapidly and linearly with increasing temperature. This indicates an increase in the level of tail disorder, and almost certainly an increase in the statistical density of *gauche* bonds, leading to tails which are, on the average, shorter.

Thus, from X-ray data alone, one would anticipate that the $K \rightarrow H$ transition involves straightening out the pair of *gauche* bonds in the K phase and an increase in the extent of tail vibrational motion, while the $H \rightarrow D_{hd}$ transition involves a rapid increase in the population of *gauche* bonds. From this viewpoint, the rapid evolution of the CH_3 stretching modes around 60°C may imply a large increase in thermal motion of the tails just below the transition temperature, followed by the two tails with *gauche* bonds straightening out when the H phase develops. Note that no dramatic change is seen at either the $H \rightarrow D_{hd}$ or $D_{hd} \rightarrow I$ transition.

While the differences in the CH_3 stretches as a function of temperature are easily observable, there is hardly any change in the frequency of the CH_2 stretching bands. The CH_2 stretching frequencies have been shown[36,37] to be sensitive only to nearby *gauche* bonds; it thus appears that *gauche* bonds are only present, if at all, near the ends of the tails. Of course, we cannot rule out the possibility of rearrangements of intensity or position in unresolved sub-bands. By contrast, the CH_3 bending modes and the benzene stretching modes show clear anomalies at the $K \rightarrow H$ and $H \rightarrow D_{hd}$ transitions. This is to be expected for the benzene breathing modes, since both of these transitions involve changes in intracolumnar ordering, and hence in core-core interactions. The CH_3 bending modes are sensitive to tail packing and conformation,[38] and thus also show clear anomalies at these transitions.

We note that no absorption bands, including those not presented in detail above, show any anomaly at the $D_{hd} \rightarrow I$ transition. From the results in the CH stretching region, we conclude that there is no sudden increase in the number of *gauche* bonds in going from the H to the D_{hd} phase, or from the D_{hd} to the I phase. The results from the benzene stretching region also suggest that the changes in the core environment in going from the D_{hd} to the I phase must be very subtle. From the plots in Figure 4, we note that although the nominal melting point of HHTT is 62°C, we observe changes in the slopes of the plots at about 50°C. Since all the frequencies shown in Figure 4 are affected by tail vibrations, this suggests that the alkyl tails actually gain considerable thermal motion at about 10°C below the nominal melting point.

In summary, our results, together with previously published X-ray data, are consistent with the following microscopic picture: Substantial evolution is seen in the K phase at about 10°C prior to melting. This effect is most likely due to increased thermal motion of the tails. (We have observed[22] similar effects in truxene derivatives HATX and HBTX: both materials show pronounced changes in the CH_2 stretching mode frequencies at their melting points. In addition, HATX shows a transition at about 20°C below the nominal melting point in which the alkyl tail gain significant disorder, as seen both in FTIR[22] and calorimetry[39] measurements.) The $K \rightarrow H$ transition in HHTT primarily involves motion of the end methyl groups. It is probable that as the amplitude of thermal vibration increases, the distribution

of environments becomes wider, and that the static *gauche* bonds found in the K phase may disappear. Microscopically, the $H \rightarrow D_{hd}$ transition primarily involves a change in core-core interactions, with no dramatic change in tail configurations. As the system is warmed in the D_{hd} phase, the density of *gauche* bonds must surely increase, but this appears to take place in a very gradual fashion. Finally, the lack of any observable anomalies in the IR spectra at the $D_{hd} \rightarrow I$ transition indicates that the two phases most likely have very similar short-range order.

Acknowledgment

We thank George Furst and John Brahms for help with the FTIR instrumentation. We also thank Professors Eugene Nixon and William Dailey for help in interpreting the complex IR spectra. This work was supported by the National Science Foundation, MRL Program, under Grant No. DMR-8819885.

References

1. S. Chandrasekhar, B. K. Sadashiva and K. A. Suresh, *Pramana*, **9**, 471 (1977).
2. A. M. Levelut, *J. Chim. Phys.*, **809**, 149 (1983).
3. C. R. Safinya, K. S. Liang, W. A. Varady, N. A. Clark and G. Anderssen, *Phys. Rev. Lett.*, **53**, 1172 (1984).
4. E. Fontes, P. A. Heiney, M. Ohba, J. N. Haseltine and A. B. Smith, *Phys. Rev.*, **A37**, 1329 (1988).
5. W. K. Lee, B. A. Wintner, E. Fontes, P. A. Heiney, M. Ohba, J. N. Haseltine and A. B. Smith, *Liq. Cryst.*, **4**, 87 (1989).
6. E. Fontes, P. A. Heiney and W. H. de Jeu, *Phys. Rev. Lett.*, **61**, 1202 (1988).
7. P. A. Heiney, E. Fontes, W. H. de Jeu, A. Riera, P. Carroll and A. B. Smith, *J. Phys. France*, **50**, 461 (1989).
8. A. M. Levelut, *J. Phys. France*, **40**, L-81 (1979).
9. A. M. Levelut, P. Oswald, A. Ghanem and J. Malthete, *J. Phys. France*, **45**, 745 (1984).
10. A. M. Levelut, J. Malthete and A. Collet, *J. Phys. France*, **47**, 351 (1986).
11. X. Yang, D. A. Waldman, S. L. Hsu, S. A. Nitzche, R. Thakur, D. M. Collard, C. P. Lillya and H. D. Stidham, *J. Chem. Phys.*, **89**, 5950 (1988).
12. V. Ruter, M. Vilfan, A. Zann and J. C. Dubois, *J. Phys. France*, **43**, 761 (1982).
13. D. Goldfarb, R. Y. Dong, Z. Luz and H. Zimmerman, *Mol. Phys.*, **54**, 1185 (1985).
14. E. Lifshitz, D. Goldfarb, S. Vega, Z. Luz and H. Zimmerman, *J. Am. Chem. Soc.*, **7280** (1987).
15. H. Toriumi, T. Shimmura, H. Watanabe and H. Saito, *Chem. Soc. Jpn.*, **61**, 2569 (1988).
16. C. L. Khetrapal, S. Raghothama, N. Suryaprakash and A. C. Kumar, *Liq. Cryst.*, **3**, 413 (1988).
17. B. Huser and H. W. Spiess, *Makr. Chem. Rapid. Commun.*, **9**, 337 (1988).
18. M. Kardan, A. Kaito, S. L. Hsu, R. Thakur and C. P. Lillya, *J. Phys. Chem.*, **91**, 1809 (1987).
19. D. P. L. Strommen, A. M. Giroud-Godquin, P. Maldivi, J. C. Marchon and B. Marchon, *Liq. Cryst.*, **2**, 689 (1987).
20. X. Yang, M. Kardan, S. L. Hsu, D. Collard, R. B. Heath and C. P. Lillya, *J. Phys. Chem.*, **92**, 196 (1988).
21. X. Yang, S. A. Nitche, S. L. Hsu, D. Collard, R. Thakur, C. P. Lillya and H. D. Stidham, *Macromolecules*, **22**, 2611 (1989).
22. W. K. Lee, P. A. Heiney, M. Ohba, J. N. Haseltine and A. B. Smith, III, *Liq. Cryst.*, **8**, 839 (1990).
23. E. F. Gramsbergen, H. J. Hoving, W. H. de Jeu, K. Praefcke and B. Kohne, *Liq. Cryst.*, **1**, 397 (1986).
24. P. Carroll, private communication.
25. B. Kohne, W. Poules and K. Praefcke, *Chemiker-Ztg.*, **108**, 113 (1983).
26. K. Praefcke, B. Kohne, W. Poules and E. Poetsch, (Merck Patent G.m.b.H.) Ger. Offen. DE 3,346,980 (Cl. C07C149/36) 04 July, 1985.
27. R. Breslow, B. Juan, R. Q. Kluttz and C. Z. Xia, *Tetrahedron*, **38**, 863 (1982).
28. L. Testaferri, M. Tingoli and M. Tiecco, *J. Org. Chem.*, **45**, 4376 (1980).

29. P. Cogolli, F. Maiolo, L. Testaferri, M. Tingoli and M. Tiecco, *J. Org. Chem.*, **44**, 2642 (1979).
30. R. M. Silverstein, G. C. Bassler and T. C. Morrill, *Spectrometric Identification of Organic Compounds*, John Wiley & Sons, 4th Ed., 1981.
31. R. G. Snyder, *J. Mol. Spectrosc.*, **4**, 411 (1960).
32. R. G. Snyder and J. H. Schachtschneider, *Spectrochim. Acta*, **19**, 85 (1963).
33. J. H. Schachtschneider and R. G. Snyder, *Spectrochim. Acta*, **19**, 117 (1963).
34. D. G. Cameron, H. L. Casal, H. H. Mantsch, Y. Boulanger and I. C. P. Smith, *Biophys. J.*, **35**, 1 (1981).
35. J. Umemura, D. G. Cameron and H. H. Mantsch, *Biochim. Biophys. Acta*, **602**, 32 (1980).
36. R. G. Snyder, S. L. Hsu and S. Krimm, *Spectrochim. Acta*, **34A**, 395 (1985).
37. I. M. Asher and I. W. Levin, *Biochim. Biophys. Acta*, **468**, 63 (1977).
38. R. G. Snyder, *J. Chem. Phys.*, **47**, 1316 (1967).
39. T. W. Warmerdam, R. J. M. Nolte, W. Drenth, J. C. van Miltenburg, D. Frenkel and R. J. J. Zijlstra, *Liq. Cryst.*, **3**, 1087 (1988).